Azimuthal P-wave attributes based fracture characterization of Paleozoic buried-hill reservoir

Zhirang Zhang, Mingjin Zhao, Hongluo Wang and Shaoguo Yang, LandOcean Energy Services Co., Ltd.*

Summary

Natural fractures often occur and play a dominate role to reservoir productivity and recovery in carbonate rocks; at the same time, 3D wide-azimuth P-wave seismic data are widely available and have found their place for fracture characterization. In the complex geology of buried-hill reservoir, we find that seismic instantaneous azimuth dependent amplitude attributes are more robust for fracture intensity and orientation characterization. We then apply the approach to one Paleozoic buried-hill reservoir in Bohai Bay Basin, east China and fractured reservoir properties we generate are well consistent with local faulting strikes and fracture density of drilled holes.

Introduction

In Bohai Bay Basin in eastern China there are many buried hills, erosional remnants from long-term exposure to weathering. The weathering created the porosity for hydrocarbon storage.

Generally, seismic waves suffer severe scattering while propagating through buried hills which are characterized of complex pore spaces for hydrocarbon, such as vugs, cracks and fractures, rather than matrix pores. And even worse, the boundary between hill-body and overlying layers is usually a regional unconformity, so it exhibits a sharp contrast in stiffness (velocity) with the overlying sediments and, consequently, high reflected amplitudes. Thus the energy that can penetrate buried hills and return to the surface is so weak that the interior of the underground-hills is poorly imaged. An even greater challenge is characterizing the fracture and karst distribution within the buried hills.

Because seismic wavelength is often 100m or more for hydrocarbon exploration, much larger than typical fracture width, aligned fractures and cracks often introduce seismic anisotropy to the rock mass. Multi-component seismic methods are the most effective way to characterize fractures because shear waves are more sensitive to anisotropy than p-waves. In particular, shear wave splitting analysis is the best method for characterizing fracture density and direction (see, for example, Crampin and Peacock, 2005). However, for a variety of reasons including cost, the use of multicomponent seismic has so far been limited. Wide azimuth P-wave reflection data, more readily available, has been used as an effective alternative solution for fracture characterization.

Rock bodies with fractures vertically aligned in a preferential direction are well known as azimuthal anisotropic media. Seismic data responding to such media exhibit azimuthal anisotropy in several aspects, such as velocity, travel-time, and amplitude attributes, and in an inverse sense, the azimuthal differences observed in these data can be analyzed to characterize fracture properties such as intensity (density) and orientation. P-wave NMO velocity or travel time is a kind of average velocity in an effective sense, so it will be influenced by overlaying layers inevitably.

Azimuthal amplitude attributes are more sensitive to anisotropy as a local response, so they show higher vertical resolution than velocity-based techniques. The approach for fracture characterization is relatively straightforward. We first calculate the seismic amplitude attributes of the partial azimuthal stacks that contain the anisotropy information. These azimuth-dependent attributes are then fitted to an ellipse, e assuming that the aligned fractures induce an elliptical anisotropy. The ellipticity is proportional to fracture intensity, and the longer axis indicates fracture orientation (Shen and Toksoz, 2000; Shen et al, 2002). In this study, we evaluate several attributes and select the instantaneous azimuthal amplitude attribute from P-wave reflection data to analyze fracture density and orientation in a buried hill reservoir in the Bohai Bay Basin.

Geology, reservoir and production data

The well CG201 penetrates a buried hill, a monadnock in the southern fault block and consists of a fairly complete Paleozoic sequence of carbonates. rock and is composed of fairly complete Paleozoic section, which is located on the downthrown side of step two of the CN fault, in the north of one depression (Wang Y. and et al, 2003). There are two major strikes of the fault system in this area, NEE and NNW (Fig. 1). The reservoir is heavily faulted and highly fractured with good secondary porosity along fractures and in vugs.

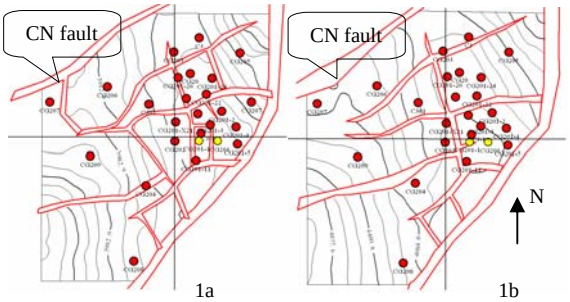

Figure 1: Structure maps of BD(a) and XM(b) formation tops.

Azimuthal P-wave attributes based fracture characterization

Undergoing multi-period tectonic movements, the monadnock reservoir interior is seriously faulted and highly fractured as well, and thus evolves into a good fractured buried hill reservoir. The reservoir of the buried hill is made of carbonate rocks where primary pores are poorly developed. Faulting and solution effects introduce considerable reservoir spaces consisting of fractures and corrosion vugs, which make commercial hydrocarbon accumulation and production possible.

The Archean and low Paleozoic formations are penetrated by the well CG201 (Fig. 2). Cuttings and logging data indicate that the oil leg is over 1495 meters long, and the petrophysical interpretation concludes that 41 oil layers add up to 245.35 m; one oil-water layer is 4.3 m; one gas layer 7.8 m and 45 dry layers 237.73 m. Oil production is up to 255 tons per day.

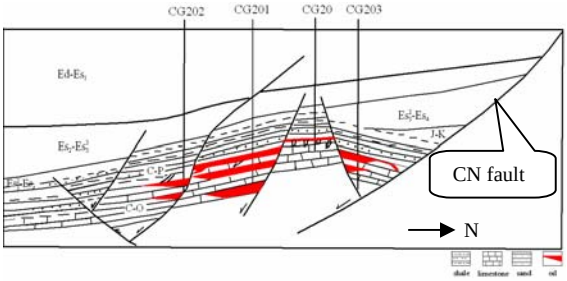

Figure 2: Sketch of CG201 buried-hill reservoir section, after Wang and et al, 2003.

Fracture characterization of CG buried hill reservoir

The offset-azimuth crossplot of the pre-stack seismic data reveal that the distribution of offset vs. azimuth is not very uniform; far-offset reflections for the range from 40 to 140 degrees were not available. We then divided the seismic data into 4 azimuthal ranges to generate 4 azimuthal partial stack data sets for fracture characterization (Fig. 3). The reflections of interest are boxed in sections with center degrees of 10, 45, 125 and 170 respectively. The dominant frequency decreases to 15Hz due to the contrast in impedance at the top of the buried hill that scatters the signal (Fig. 4).

We tested several seismic attributes such as amplitude, impedance, and instantaneous envelope, and selected instantaneous envelope to fit the anisotropy ellipse for its effectiveness in this low S/N ratio area. From the ellipse we obtain the dominant direction and relative density of the fracturing. These data are then checked against log and core data where available.

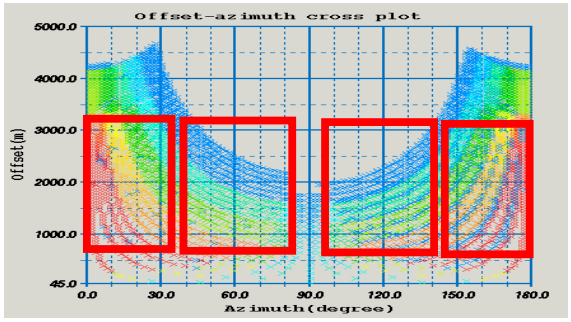

Figure 3: Offset-azimuth crossplot and divisions of partial azimuth stack.

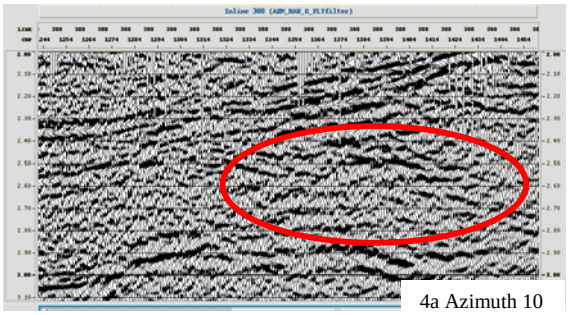

4a Azimuth 10

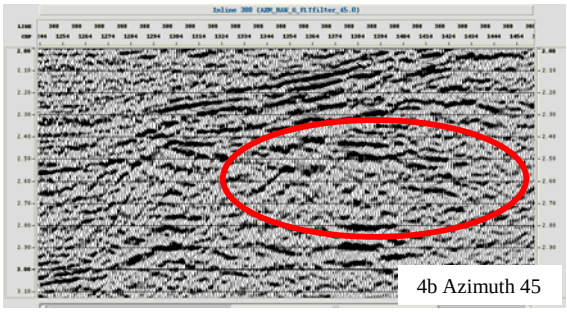

4b Azimuth 45

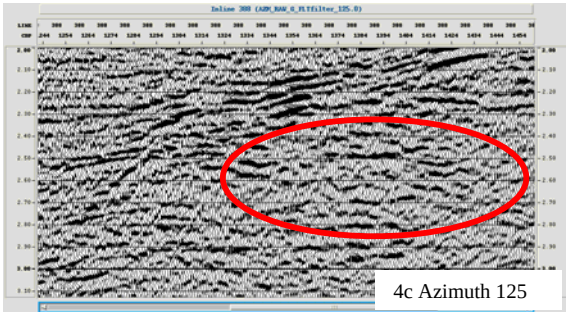

4c Azimuth 125

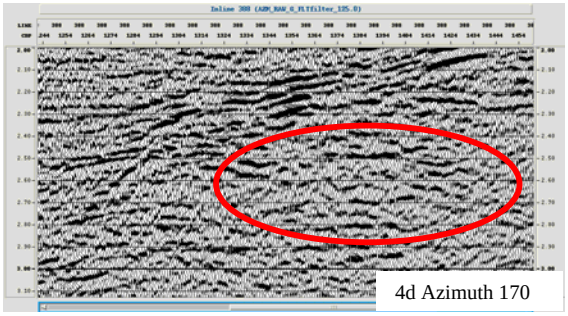

Figure 4: Azimuth sections of degree 10, 45, 125 and 170 in order, and the circled buried-hill body. The dominant frequency is almost 15 Hz.

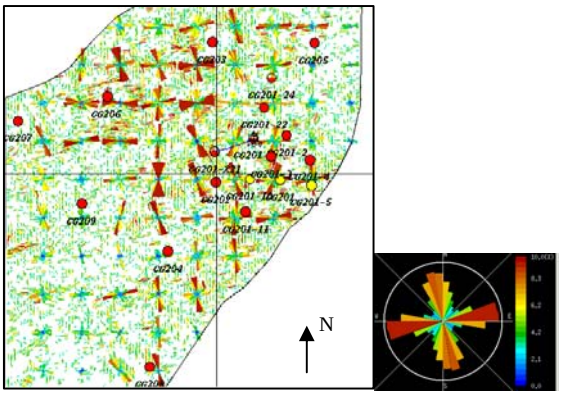

5a 5b

Figure 5: Fracture orientation local and statistical distributions.

The predicted fracture directions vary considerably locally, but group into a roughly orthogonal pattern striking ENE and NNW when all data are combined, parallel to the strikes of the faults in the area (Fig. 5). The fracture density data can be derived from fitted ellipticities for every CDP. With top and bottom horizons well constrained and a threshold of ellipticity for interpreting zones of high fracture density defined, the time thickness isograms of the BD and SM formations can be mapped. The fracture densities for BD and SM Group are mapped in figure 6 and figure 7, respectively.

Total thickness of fractured section for the BD and SM groups are determined from the seismic velocity data and compared with total length of fractured well bore as determined from the logging data (Fig. 8). The thickness of fractured well bore data was determined from resistivity logs calibrated for permeability—values greater than 0.3 are considered as sufficiently fractured to constitute reservoir. The thicknesses of fractured zones obtained from seismic compares well with the data obtained from logging (Fig. 8). We interpret the favorable comparison of the two very different methods as an indication that the seismic techniques are providing reliable data.

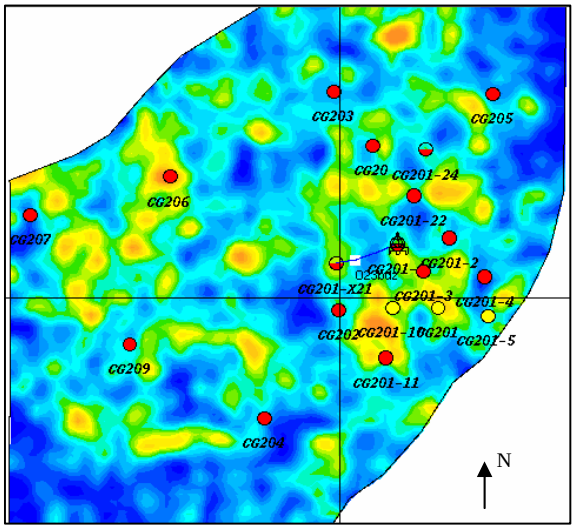

Figure 6: Fracture density of BD Group (Areas of high fracture density is warm-colored.)

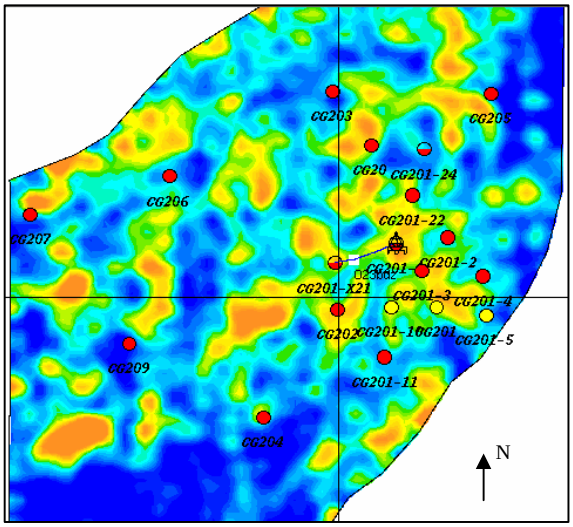

Figure 7: Fracture density of SM Group (Areas of high fracture density is warm-colored.)

As shown in figure 9, wells CG203, CG205 and CG207 are in areas where the ellipticity and, therefore, the fracture density is low Wells CG201 and CG204 are in areas where the fracture density is predicted from the seismic to be high. Production data indicate wells CG201 and CG204 are more productive than wells CG202, CG208 and CG209. CG206

produces water, and CG203, CG205 and CG207 are not productive.

Fractures are poorly developed in the northern area around well CG203 and at and east of well CG205. However, well CG205 is at the edge of a more highly fractured area and it may be possible to sidetrack into that region. Well CG204 appears to cut a fault separating a poorly fractured block to the south from a more highly fractured block to the north. That well is productive, possibly due to intersecting fractures associated with the fault. The distribution of areas of high fracture density shows some tendency to favor the structurally higher blocks. Within each bock fracture density varies rapidly but does show some tendency to connect laterally with other zones. Whether or not this is related to sub-seismic faulting is not clear.

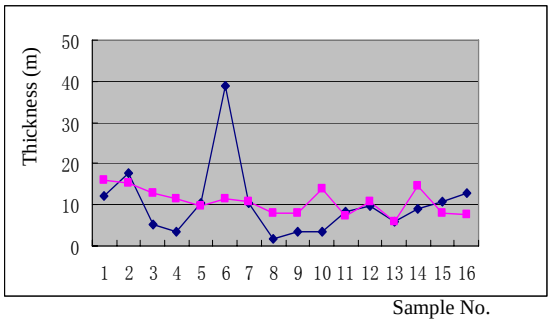

Figure 8: Seismic and logging thicknesses of fractured segments at well sites; values are derived from logging data in blue and those from p-wave seismic data in pink.

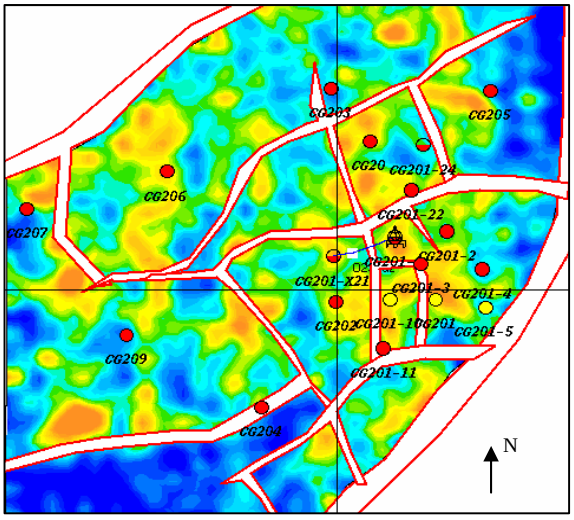

Figure 9: Total thickness of effective fractured segments of the two groups; areas of high fracture density is warm-colored.

Discussions and conclusions

Although the fractured zones appear to be distributed somewhat randomly in map view (Fig. 9), the distribution of highly fractured zones y displays more order when viewed stereoscopically (Fig. 10), where the zones appear aligned at the top of the structure and along inflections at the secondary fault terraces of the structure. Whether these zones of high density correspond to faults or regions of high curvature (strain) is not clear from the data. Both are associated with high fracture density. Whatever the cause, there is an association between seismically-determined ellipticity (anisotropy) and production. The azimuthal P-wave based fracture detection technique shows promise as a method for locating zones of high fracture density and, therefore, reducing drilling risk in this buried hill.

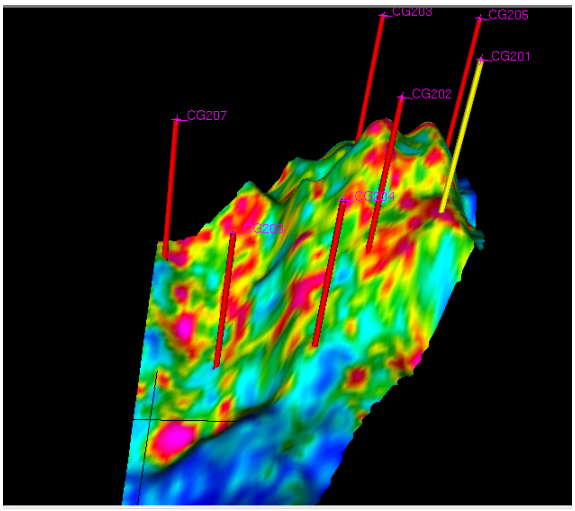

Figure 10: Total thickness of effective fractured segments of the two groups; areas of high fracture density is warm-colored.

Acknowledgments

The authors appreciate William D. Rizer's for reviewing the manuscript. And we would like to thank Miss Shuqin Sun and Miss Yanhua Guan for their excellent work preparing the illustrations and the manuscript.